Confusing nonstandard neutrino interactions with oscillations at a neutrino factory

P. Huber*

Theoretische Physik, Physik Department, Technische Universität München, James-Franck-Strasse, D-85748 Garching, Germany
and Max-Planck-Institut für Physik, Postfach 401212, D-80805 München, Germany

T. Schwetz[†] and J. W. F. Valle[‡]

Instituto de Física Corpuscular–C.S.I.C., Universitat de València, Edificio Institutos, Aptdo. 22085, E-46071 València, Spain

Most neutrino mass theories contain nonstandard interactions (NSI) of neutrinos which can be either non-universal (NU) or flavor changing (FC). We study the impact of such interactions on the determination of neutrino mixing parameters at a neutrino factory using the so-called "golden channels" $\overset{(-)}{\nu}_e \to \overset{(-)}{\nu}_\mu$ for the measurement of θ_{13}. We show that a certain combination of FC interactions in neutrino source and earth matter can give exactly the same signal as oscillations arising due to θ_{13}. This implies that information about θ_{13} can only be obtained if bounds on NSI are available. Taking into account the existing bounds on FC interactions, this leads to a drastic loss in sensitivity in θ_{13}, at least two orders of magnitude. A near detector at a neutrino factory offers the possibility to obtain stringent bounds on some NSI parameters. Such a near site detector constitutes an essential ingredient of a neutrino factory and a necessary step towards the determination of θ_{13} and subsequent study of leptonic CP violation.

I. INTRODUCTION

From the long-standing solar [1] and atmospheric [2] neutrino anomalies we now have compelling evidence that an extension of the standard model (SM) of particle physics is necessary in the lepton sector. The simplest and most generic explanation of these experiments is provided by neutrino oscillations induced by neutrino masses and mixing. As is well known and accepted, the indication of the Liquid Scintillation Neutrino Detector (LSND) experiment [3] for oscillations at a large mass-squared difference cannot be reconciled with solar and atmospheric data within a 3-neutrino framework. For recent four-neutrino [4] analyses see Ref. [5] and references therein. For this reason we choose not to consider the LSND data and focus therefore on the simplest 3-neutrino scheme with the two mass-squared differences $\Delta m_{\text{sol}}^2 \lesssim 10^{-4}$ eV^2 and $\Delta m_{\text{atm}}^2 \approx 3 \times 10^{-3}$ eV^2 [6]. The corresponding lepton mixing matrix is parametrized by the three angles $\theta_{12}, \theta_{23}, \theta_{13}$ and one complex CP-violating phase δ (see later for exact definitions) relevant in lepton-number-conserving neutrino oscillations [7,8]. It is known from atmospheric neutrino data that θ_{23} has to be nearly maximal. On the other hand, data from present solar neutrino experiments favor a large value for the angle θ_{12} [9,10]. An improved determination is expected from solar neutrino data and/or the results of the KamLAND experiment [11]. The value of the third angle θ_{13} is not known at present, there is only the bound

$$\sin^2 2\theta_{13} \lesssim 0.1 \quad \text{at} \quad 90\% \text{ C.L.} \tag{1}$$

implied by combining the results of the reactor experiments [12] CHOOZ and Palo Verde with atmospheric data. Together with the requirement of solar neutrino oscillations this bound implies that $\sin^2 \theta_{13}$ has to be small. The value of the phase δ is completely unknown.

Currently a new generation of long-baseline neutrino oscillation experiments using a neutrino beam originating from the decay of muons in a storage ring is being discussed [13]. These so-called *neutrino factories* are considered as the ideal tool to enhance our knowledge about neutrino mixing parameters. In addition to the possibility to explore CP violation in the lepton sector an important aim of a neutrino factory will be a precise determination of θ_{13}; it is claimed that a measurement of θ_{13} down to values of a few$\times 10^{-4}$ will be possible [14].

In a large class of models beyond the standard model nonstandard interactions (NSI) of neutrinos with matter arise. The simplest NSI do not require new interactions beyond those mediated by the standard model electroweak gauge bosons: it is simply the nature of the leptonic charged and neutral current interactions which is nonstandard due to the complexity of neutrino mixing [7]. On the other hand NSI can also be mediated by the exchange of new particles with mass at the weak scale such as in some supersymmetric models with R-parity violating [15,16] interactions. Such nonstandard flavor-violating physics can arise even in the absence of neutrino mass [17,18] and can lead to nonuniversal (NU) or to flavor-changing (FC) neutrino interactions.

Nonstandard interactions of neutrinos affect their propagation in matter and the magnitude of the effect depends on the interplay between conventional mass-induced neutrino oscillation features in matter [19] and those genuinely engendered by the NSI, which do not require neutrino mass [20]. Correspondingly their implications have been explored in a variety of contexts involving solar neutrinos [19–23], atmospheric neutrinos [23–26], other astrophysical sources

*Electronic address: Patrick.Huber@ph.tum.de
[†]Electronic address: schwetz@ific.uv.es
[‡]Electronic address: valle@ific.uv.es

[27,28] and the LSND experiment [29,30]. The impact of nonstandard interactions of neutrinos has also been considered from the point of view of future experiments involving solar neutrinos [31] as well as the upcoming neutrino factories [32,33]. Various aspects of NSI for a neutrino factory experiment have been considered in Refs. [32–39].

In this paper we will consider from a phenomenological point of view the impact of NSI on the determination of neutrino mixing parameters at a neutrino factory. In particular we will focus on the $\overset{(-)}{\nu}_e \to \overset{(-)}{\nu}_\mu$ channels, which are supposed to be the "golden channels" for the measurement of θ_{13}. We extend our previous work [33] by taking simultaneously into account neutrino oscillations and the effect of NSI in neutrino source, propagation and detection [38]. We will show that a certain combination of FC interactions in source and propagation can give exactly the same signal as oscillations arising due to θ_{13}. This implies that information about θ_{13} can only be obtained if bounds on NSI are available. In view of the existing bounds on FC interactions, this leads to a drastic loss in sensitivity in θ_{13}, at least two orders of magnitude.

All our considerations also apply to the determination of θ_{13} in long baseline experiments using upgraded conventional beams [38,40]. However, due to the different production processes involved, the NSI parameters relevant in the source of a conventional beam experiment differ from the ones at a neutrino factory. The same methods discussed here can be adapted to cover that case also. A detailed numerical consideration of conventional beam experiments goes beyond the scope of this work.

The outline of the paper is as follows. In Sec. II we briefly sketch the theoretical motivation for NSI in the context of gauge theories of neutrino mass. In Sec. III we discuss examples of low energy four-fermion Hamiltonians, which lead to NSI in neutrino source, propagation and detection. In Sec. IV we review some bounds on NSI parameters obtained in the literature. In Sec. V we present the framework of our numerical calculations and discuss the appearance rate in the presence of NSI and oscillations. In Sec. VI we derive analytical expressions for this rate and formulate the *oscillation-NSI confusion theorem*. In Sec. VII we describe the simulation of a neutrino factory and our statistical method to investigate the possibilities of such an experiment to determine NSI and oscillation parameters. In Sec. VIII we define sensitivity limits for $\sin^2 2\theta_{13}$ and show our numerical results for the three baselines 700 km, 3000 km and 7000 km as a function of bounds on the relevant NSI parameters. We also discuss the sensitivity limits if information from two different baselines is combined. Finally we conclude in Sec. IX.

II. THEORETICAL MOTIVATION

More often than not, models of neutrino mass are accompanied by NSI, leading generically to both oscillations and neutrino NSI in matter. The simplest are those NSI which arise from neutrino-mixing. The most straightforward example of this case is when neutrino masses follow from the admixture of isosinglet neutral heavy leptons as, for example, in seesaw schemes [41]. These contain $SU(2)$

$\otimes U(1)$ singlets with a gauge invariant Majorana mass term of the type $M_{Rij} \nu_i^c \nu_j^c$ which breaks total lepton number symmetry, perhaps at a large $SO(10)$ or left-right breaking scale. The masses of the light neutrinos are obtained by diagonalizing the mass matrix

$$\begin{bmatrix} M_L & D \\ D^T & M_R \end{bmatrix} \tag{2}$$

in the basis ν, ν^c, where D is the standard $SU(2) \otimes U(1)$ breaking Dirac mass term, and $M_R = M_R^T$ is the large isosinglet Majorana mass and the $M_L \nu \nu$ term is an isotriplet [7]. In left-right models the latter is generally suppressed as $M_L \propto 1/M_R$.

The structure of the associated effective weak $V-A$ currents is rather complex [7]. The first point to notice is that the heavy isosinglets will mix with the ordinary isodoublet neutrinos in the charged current weak interaction. As a result, the mixing matrix describing the charged leptonic weak interaction is a rectangular matrix K [7] which may be decomposed as

$$K = (K_L, K_H) \tag{3}$$

where K_L and K_H are 3×3 matrices. The corresponding neutral weak interactions are described by a nontrivial matrix [7]

$$P = K^\dagger K. \tag{4}$$

In such models nonstandard interactions of neutrinos with matter arise from the non-trivial structures of the charged and neutral weak currents. Note, however, that the smallness of neutrino mass, which follows due to the seesaw mechanism $M_{\nu \text{eff}} = M_L - D M_R^{-1} D^T$ and the condition

$$M_L \ll M_R, \tag{5}$$

implies that the magnitude of neutrino NSI is expected to be negligible. However this need not be so in general. For example, since the number m of $SU(2) \otimes U(1)$ singlets is arbitrary, one may consider models with Majorana neutrinos based on *any value* of m. One can therefore extend the lepton sector of the $SU(2) \otimes U(1)$ theory by adding a set of *two* 2-component isosinglet neutral fermions, denoted ν_i^c and S_i, in each generation [17]. In such $m=6$ models one can consider the 9×9 mass matrix [42]

$$\begin{bmatrix} 0 & D & 0 \\ D^T & 0 & M \\ 0 & M^T & \mu \end{bmatrix} \tag{6}$$

(in the basis ν, ν^c, S). The Majorana masses for the neutrinos are determined from

$$M_L = D M^{-1} \mu M^{T-1} D^T. \tag{7}$$

In the limit $\mu \to 0$ the exact lepton number symmetry is recovered and neutrinos become massless [17]. This provides an elegant way to generate neutrino masses without a super-

heavy scale and automatically allows one to enhance the magnitude of neutrino NSI strengths by avoiding the constraints which arise from the smallness of neutrino masses presently indicated by the oscillation interpretation of solar and atmospheric neutrino data.

The propagation of the light neutrinos is effectively described by a truncated mixing matrix K_L which is not unitary. This may lead to oscillation effects in matter, even if neutrinos were massless [20]. They may be resonant and therefore important in supernovae matter [20,27]. The strength of NSI is hence unrestricted by the magnitude of neutrino masses, only by universality limits, and may be large, at the few percent level. The phenomenological implications of these models have been widely investigated [43–47].

An alternative way to induce neutrino NSI is in the context of the most general low-energy super-symmetry model, without R-parity conservation [15]. In addition to bilinear violation [16,48] one may also have trilinear L violating couplings in the super-potential

$$\lambda_{ijk} L_i L_j E_k^c \tag{8}$$

$$\lambda'_{ijk} L_i Q_j D_k^c \tag{9}$$

where L, Q, E^c and D^c are (chiral) super-fields which contain the usual lepton and quark $SU(2)$ doublets and singlets, respectively, and i,j,k are generation indices. The couplings in Eq. (8) give rise at low energy to the following four-fermion effective Lagrangian for neutrinos interactions with d-quark including

$$\mathcal{L}_{\text{eff}} = -2\sqrt{2} G_F \sum_{\alpha,\beta} \xi_{\alpha\beta} \bar{\nu}_{L\alpha} \gamma^\mu \nu_{L\beta} \bar{d}_R \gamma^\mu d_R,$$

$$\alpha,\beta = e,\mu,\tau, \tag{10}$$

where the parameters $\xi_{\alpha\beta}$ represent the strength of the effective interactions normalized to the Fermi constant G_F. One can identify explicitly, for example, the following *nonstandard* flavor-conserving NSI couplings

$$\xi_{\mu\mu} = \sum_j \frac{|\lambda'_{2j1}|^2}{4\sqrt{2} G_F m_{\tilde{q}_{jL}}^2}, \tag{11}$$

$$\xi_{\tau\tau} = \sum_j \frac{|\lambda'_{3j1}|^2}{4\sqrt{2} G_F m_{\tilde{q}_{jL}}^2}, \tag{12}$$

and the FC coupling

$$\xi_{\mu\tau} = \sum_j \frac{\lambda'_{3j1} \lambda'_{2j1}}{4\sqrt{2} G_F m_{\tilde{q}_{jL}}^2} \tag{13}$$

where $m_{\tilde{q}_{jL}}$ are the masses of the exchanged squarks and $j = 1,2,3$ denotes $\tilde{d}_L, \tilde{s}_L, \tilde{b}_L$, respectively. The existence of effective neutral current interactions contributing to the neutrino scattering off d-quarks in matter, provides new flavor-conserving as well as flavor-changing terms for the matter

potentials of neutrinos. Such NSI are directly relevant for solar and atmospheric neutrino propagation [23].

Clearly, such neutrino NSI are accompanied by nonzero neutrino masses. In fact one has a hybrid model for neutrino masses in which the atmospheric scale arises at the tree level while the solar neutrino scale is induced by loops which involve directly the NSI coefficients in Eq. (8). This way one obtains the co-existence of oscillations as well as NSI of neutrinos. The relative importance of NSI and oscillation features is parameter-dependent.

An alternative variant of the above scheme is provided by some radiative models of neutrino masses such as the one discussed in [49]. In all such models NSI may arise from scalar interactions.

Finally, we mention that unification provides an alternative and elegant way to induce neutrino NSI. For example unified super-symmetric models lead to NSI as a result of super-symmetric scalar lepton non-diagonal vertices induced by renormalization group evolution [18,50]. In the special case of $SU(5)$ the NSI may exist without neutrino mass. In $SO(10)$ neutrino masses co-exist with neutrino NSI.

In what follows we shall investigate the interplay of NSI-induced and neutrino-mass-induced (oscillation-induced) conversion of neutrinos at a neutrino factory and on how it can vitiate the otherwise very precise determination of neutrino oscillation parameters.

III. EFFECTIVE FOUR-FERMION HAMILTONIANS DESCRIBING NSI

In this section we consider in some detail the simplest examples of effective low energy Hamiltonians, which lead to NSI in the source (S), propagation (P) and detection (D) of neutrinos in a neutrino factory experiment.

In such an experiment neutrinos are produced by the decay of the stored muons $\mu^+ \to e^+ + \nu_e + \bar{\nu}_\mu$ and the charge conjugated process. In the SM these processes are described by the effective four-fermion Hamiltonian

$$\mathcal{H}_{\text{SM}}^S = \frac{G_F}{\sqrt{2}} [\bar{\nu}_\mu (1-\gamma_5) \gamma_\lambda \mu][\bar{e}(1-\gamma_5) \gamma^\lambda \nu_e] + \text{H.c.} \tag{14}$$

In addition to this SM term, resulting from the exchange of the W boson, we consider now new processes $\mu^+ \to e^+ + \nu_\alpha + \bar{\nu}_\mu$ with any flavor $\alpha = e,\mu,\tau$ for the neutrino related to the positron.[1] We parametrize the corresponding NSI effective Hamiltonian by the coefficients $\epsilon_{e\alpha}^S$:

---

[1] In this work we will consider the $e \to \mu$ appearance channel and hence, we are interested only in the neutrino produced together with the positron (or the electron, for the charge conjugated processes). More generally, also processes $\mu^+ \to e^+ + \nu_\alpha + \bar{\nu}_\beta$ with an arbitrary flavor combination $(\alpha,\beta) = (e,\mu,\tau)$ may occur. In this case the final state in the source can be different from the one in the SM. Such additional processes must be added incoherently to obtain the transition rate defined later in Eq. (26). For simplicity we will not consider this possibility further.

$$\mathcal{H}_{\mathrm{NSI}}^{S}=\frac{G_F}{\sqrt{2}}[\bar{\nu}_\mu(1-\gamma_5)\gamma_\lambda\mu]\sum_\alpha \epsilon_{e\alpha}^{S}[\bar{e}(1-\gamma_5)\gamma^\lambda\nu_\alpha]+\mathrm{H.c.}$$

$$(15)$$

Note that the value of the SM Fermi constant G_F is determined experimentally from the decay width of the muon [51], without measuring the flavor of the neutrinos. Therefore, we have the relation

$$G_F^{\mathrm{exp}}=G_F\left(|1+\epsilon_{ee}^{S}|^2+\sum_{\alpha=\mu,\tau}|\epsilon_{e\alpha}^{S}|^2\right)^{1/2}. \qquad (16)$$

The term ϵ_{ee}^{S} leads to exactly the same final state as the SM process and must be added coherently, whereas $\epsilon_{e\mu}^{S}$ and $\epsilon_{e\tau}^{S}$ lead to different final states and contribute incoherently to the decay. From Eq. (16) one learns that the high precision measurement of G_F^{exp} on its own (within an accuracy of 9×10^{-6} [51]) does not constrain any of the parameters in the Hamiltonian G_F and $\epsilon_{e\alpha}^{S}$ directly [52]; only the *combination* shown in Eq. (16) is constrained within the accuracy of the experimental measurement.

The standard muon detectors under discussion for a neutrino factory experiment make use of charged current processes like $\nu_\mu+d\to\mu^-+u$. The relevant effective Hamiltonian in the SM is given by

$$\mathcal{H}_{\mathrm{SM}}^{D}=\frac{G_F}{\sqrt{2}}[\bar{d}(1-\gamma_5)\gamma_\lambda u][\bar{\nu}_\mu(1-\gamma_5)\gamma^\lambda\mu]+\mathrm{H.c.}$$

$$(17)$$

Here $d(u)$ symbolizes any down-(up-)type quark. Similar to Eq. (15) we consider the following NSI four-fermion Hamiltonian:

$$\mathcal{H}_{\mathrm{NSI}}^{D}=\frac{G_F}{\sqrt{2}}[\bar{d}(1-\gamma_5)\gamma_\lambda u]\sum_\alpha \epsilon_{\alpha\mu}^{D}[\bar{\nu}_\alpha(1-\gamma_5)\gamma^\lambda\mu]+\mathrm{H.c.}$$

$$(18)$$

The coefficients $\epsilon_{\alpha\mu}^{D}$ describe NU ($\alpha=\mu$) or FC ($\alpha=e,\tau$) NSI in the detector, *e.g.* a nonzero $\epsilon_{\tau\mu}^{D}$ leads to the process $\nu_\tau+d\to\mu^-+u$.

In a long-baseline neutrino experiment a significant part of the neutrino path will cross the earth and hence neutrino NSI with earth matter must be taken into account. Let us consider the effective Hamiltonian describing the SM neutral current processes of neutrinos with a fermion f due to the exchange of the Z boson $\nu_\alpha+f\to\nu_\alpha+f$:

$$\mathcal{H}_{\mathrm{SM}}^{P}=\frac{G_F}{\sqrt{2}}[\bar{f}(g_V^f-g_A^f\gamma_5)\gamma_\lambda f]\sum_\alpha [\bar{\nu}_\alpha(1-\gamma_5)\gamma^\lambda\nu_\alpha],$$

$$(19)$$

where g_V^f and g_A^f are the SM vector and axial couplings of the fermion f, see, e.g., Ref. [51], Sec. 10. In the SM this interaction is the same for all flavors and hence, has no effect on the propagation of the neutrino state—in contrast to the charged current interaction of $\overset{(-)}{\nu}_e$ with electrons. However, if

NSI are present, we must also take into account processes $\nu_\alpha+f\to\nu_\beta+f$ with arbitrary flavor combinations ($\alpha\beta$) described by the Hamiltonian

$$\mathcal{H}_{\mathrm{NSI}}^{P}=\frac{G_F}{\sqrt{2}}[\bar{f}(g_V^f-g_A^f\gamma_5)\gamma_\lambda f]\sum_{\alpha\beta} \epsilon_{\alpha\beta}^{f}[\bar{\nu}_\alpha(1-\gamma_5)\gamma^\lambda\nu_\beta].$$

$$(20)$$

In Eqs. (15),(18),(20) we have assumed for simplicity, that the NSI have the same $V-A$ Lorentz structure as the SM interactions. This need not be the case in the most general extension of the SM involving, say, left-right symmetry, where many new NSI parameters can appear (see e.g. Refs. [37,38]). However, the effects of NSI with $V+A$ Lorentz structure are strongly suppressed since the left-right breaking scale should be rather high in order to account for the smallness of the neutrino masses indicated by solar and atmospheric experiments. Moreover, one expects that only certain combinations of parameters will be relevant for the experimental configuration we are considering here, and for any given theory our results can be mapped to the corresponding combination of parameters.

Although different processes are relevant for source, propagation and detection, in a given model relations between the coefficients $\epsilon_{\alpha\beta}^{X}$ may exist. However, such relations highly depend on the underlying model. In order to be model-independent we will treat all $\epsilon_{\alpha\beta}^{X}$ as independent parameters.

IV. BOUNDS ON NSI PARAMETERS

In this section we review existing bounds on neutrino NSI obtained in the literature. The most direct upper bounds on the strength of NSI interactions arise from negative searches for neutrino oscillations [37,53,54]. For example the bounds on the transition probabilities $P_{\nu_\mu\to\nu_\tau}\lesssim3.4\times10^{-4}$ and $P_{\nu_e\to\nu_\tau}\lesssim2.6\times10^{-2}$ obtained by CHORUS [55] yield the bounds

$$|\epsilon_{\mu\tau}^{\mathrm{CHORUS}}|\lesssim1.8\times10^{-2}, \quad |\epsilon_{e\tau}^{\mathrm{CHORUS}}|\lesssim0.16. \qquad (21)$$

With the superscript we indicate that the constrained quantity actually is a certain combination of NSI coefficients relevant in the neutrino source and detection processes for a given experiment [see later Eq. (33)], which in general is different from the NSI coefficients relevant for neutrino factory experiments.

Recently, in Ref. [25] the strong evidence for oscillations of atmospheric neutrinos has been used to set upper bounds on NSI of neutrinos with the down quarks in earth matter:

$$|\epsilon_{\mu\tau}^{d}|\lesssim3\times10^{-2}, \quad |\epsilon_{\tau\tau}^{d}|\lesssim6\times10^{-2}. \qquad (22)$$

Similar bounds on the magnitude of neutrino NSI with electrons and up-type quarks may be derived [23].

Besides these direct bounds on neutrino NSI there is a lot of data constraining non-standard effects in *charged lepton* processes. However, it is very nontrivial in general to use

these data to derive model-independent bounds on neutrino NSI coefficients. For a recent discussion see, for example, Refs. [26,29,35]. To obtain such bounds for neutrino interactions one must convert from the bounds on charged lepton processes making some assumption about $SU(2)_L$ symmetry. In Ref. [22] the corresponding bounds for the charged leptons are multiplied by a factor of ≈ 6.8, in order to take into account $SU(2)_L$ breaking effects. In this way the following bounds on neutrino NSI are derived from pure leptonic processes [22]:

$$|\epsilon^\ell_{e\mu}| \lesssim 7 \times 10^{-6}, \quad |\epsilon^\ell_{e\tau}| \lesssim 3 \times 10^{-2}. \tag{23}$$

As the neutrino production in a neutrino factory is also a pure leptonic process we take the bounds (23) as order of magnitude estimates of the NSI at the neutrino source. From bounds on $\mu \to e$ conversion in muon scattering off nuclei and from those on flavor-violating hadronic tau decays the following bounds on neutrino NSI with quarks are derived [22]:

$$|\epsilon^q_{e\mu}| \lesssim 7 \times 10^{-5}, \quad |\epsilon^q_{e\tau}| \lesssim 7 \times 10^{-2}. \tag{24}$$

We take this as an order of magnitude estimate for the NSI in propagation and detection at a neutrino factory experiment, since there also processes with quarks are involved. For the $\mu - \tau$ channel the bounds are of order [26]

$$|\epsilon_{\mu\tau}| \lesssim 5 \times 10^{-2} \tag{25}$$

and for the NU coefficients upper bounds of order 0.1 are derived.

However, in Ref. [56] it has been stressed that in general no model-independent relation exists between NSI coefficients for charged leptons and neutrinos and only much weaker bounds of order 50% are derived using data from $e^+ e^-$ colliders. This more conservative viewpoint has been exploited to show how FC neutrino interactions provide an excellent description of the solar neutrino data, while consistent with the oscillation description of the atmospheric data [23].

V. THE APPEARANCE RATE IN A NEUTRINO FACTORY EXPERIMENT

Let us consider the impact of NSI in source, propagation and detection on the $e \to \mu$ channel[2] at a neutrino factory. Starting from the decay of a μ^+, we make the following ansatz for the rate at which a neutrino produced together with the positron leads to the production of a μ^- in the detector [38]:

$$\mathcal{R}_{e\mu} = \left| \sum_{\alpha\beta} \mathcal{A}^S_{e\alpha} \mathcal{A}^P_{\alpha\beta} \mathcal{A}^D_{\beta\mu} \right|^2, \tag{26}$$

---

[2]For the sake of clarity we keep the oscillation-inspired terminology "$e \to \mu$ appearance channel" ("$\mu \to \mu$ disappearance channel"). We actually mean the production of a wrong-sign (like-sign) muon in the detector, respectively.

and similar for the charge conjugated process. Here we define the amplitudes describing the neutrino source and detection process as

$$\mathcal{A}^X_{\alpha\beta} \equiv \delta_{\alpha\beta} + \epsilon^X_{\alpha\beta} \quad \text{for} \quad X = S, D, \tag{27}$$

and the amplitude $\mathcal{A}^P_{\beta\gamma}$ describes the propagation of the neutrino state from the production point to the detector. This amplitude is obtained from the solution of a Schrödinger equation with the Hamiltonian

$$H_\nu = \frac{1}{2E_\nu} U \text{diag}(0, \Delta m^2_{\text{sol}}, \Delta m^2_{\text{atm}}) U^\dagger$$

$$+ \text{diag}(V, 0, 0) + \sum_f V_f \epsilon^f, \tag{28}$$

which takes into account neutrino oscillations and SM interactions as well as NSI with the matter crossed by the neutrino beam. Here E_ν is the neutrino energy and $V = \sqrt{2} G_F N_e$ is the matter potential due to the SM charged current interaction [19], where N_e is the electron number density. The last term in Eq. (28) describes the NSI with earth matter. The sum is over all fermions f present in matter, and $V_f \epsilon^f_{\alpha\beta}$ is the coherent forward scattering amplitude of the process $\nu_\alpha + f \to \nu_\beta + f$, where $V_f = \sqrt{2} G_F N_f$, with the number density of the fermion f along the neutrino path given by N_f. We define an effective NSI coefficient for the propagation by normalizing all contributions to the down-quark potential V_d:

$$\epsilon^P_{\alpha\beta} \equiv \sum_f \frac{V_f}{V_d} \epsilon^f_{\alpha\beta}. \tag{29}$$

Adopting a basis where the charged lepton mass matrix is diagonal, the unitary matrix U in Eq. (28) relates the neutrino fields in the basis where the neutrino mass matrix is diagonal to the neutrino fields in the basis where the interaction with the SM W boson is diagonal [53]. We parametrize this matrix in the following way [7]:

$$U = U_{23} U_{13} U_{12} = \begin{pmatrix} 1 & 0 & 0 \\ 0 & c_{23} & s_{23} \\ 0 & -s_{23} & c_{23} \end{pmatrix} \begin{pmatrix} c_{13} & 0 & s_{13} \\ 0 & 1 & 0 \\ -s_{13} & 0 & c_{13} \end{pmatrix}$$

$$\times \begin{pmatrix} c_{12} & e^{i\delta} s_{12} & 0 \\ -e^{-i\delta} s_{12} & c_{12} & 0 \\ 0 & 0 & 1 \end{pmatrix}, \tag{30}$$

where $s_{ij} = \sin\theta_{ij}$ and $c_{ij} = \cos\theta_{ij}$.

In this paper we consider the following simplified scenario. First, we take all $\epsilon^X_{\alpha\beta}$ real and we assume that they are the same for neutrinos and anti-neutrinos as in [25]. Second, Eqs. (23) and (24) suggest that constraints on FC interactions

in the $e - \mu$ channel are about 3 orders of magnitude stronger than in the other channels. This motivates the approximation[3]

$$\epsilon_{e\mu}^X \approx \epsilon_{\mu e}^X \approx 0 \quad \text{for} \quad X = S, P, D. \quad (31)$$

Third, we neglect the solar mass-squared difference, which implies also that the angle θ_{12} and the phase δ disappear [7]. Then we are left with the following neutrino propagation Hamiltonian:

$$H_\nu = U_{23} U_{13} \text{ diag } (0,0,\Delta) U_{13}^\dagger U_{23}^\dagger + \text{diag}(V,0,0) + Vr\epsilon^P, \quad (32)$$

where we have defined $\Delta \equiv \Delta m_{\text{atm}}^2 / 2E_\nu$ and $r \equiv V_d / V = N_d / N_e$ with $r \approx 3$ in earth matter. In the Hamiltonian (32) a sign change of Δ is equivalent to a sign change of V, which interchanges the evolution of neutrinos and anti-neutrinos. Therefore, it is sufficient to consider only the case $\Delta > 0$, assuming that the neutrino factory is run in both polarities.

A detector close to the front end of a neutrino factory—a so-called *near detector*—can be a very powerful tool to constrain NSI [36,39,57]. Such a detector has to be situated at a short distance (a few 100 m) from the production region of the neutrinos, such that no oscillations with Δm_{atm}^2 or Δm_{sol}^2 can develop and matter effects are negligible. In our formalism this means that $\mathcal{A}_{\alpha\beta}^P = \delta_{\alpha\beta}$, and the transition rate relevant for a near detector is simply given by

$$\mathcal{R}_{\alpha\beta}^{\text{ND}} = \left| \sum_\gamma \mathcal{A}_{\alpha\gamma}^S \mathcal{A}_{\gamma\beta}^D \right|^2. \quad (33)$$

It is clear that a near detector cannot provide any model-independent information on $\epsilon_{\alpha\beta}^P$, and only a *combination* of $\epsilon_{\alpha\beta}^S$ and $\epsilon_{\alpha\beta}^D$ is constrained.

Some remarks are in order. Although the general motivation for NSI is that these accompany models of neutrino mass generation, in our following phenomenological studies we will restrict our attention only to total lepton number conserving NSI. While this will suffice to make our point, it will on the other hand greatly simplify our analysis. This happens because in this particular case it is possible to distinguish the neutrino produced together with the electron from the one produced together with the muon, if the detector can determine the charge of the muon. We insist, however, that in a generic theory for NSI and neutrino masses also lepton number violating processes [30,39] are expected, due to the Majorana nature of neutrinos (see Sec. II). Such effects would be an additional source for the confusion of NSI and oscillations.

The off-diagonal elements $\epsilon_{\alpha\beta}^X$ ($X = S, P, D$) with $\alpha \neq \beta$ describe FC, whereas the diagonal elements with $\alpha = \beta$ lead to NU. In Eqs. (26) and (33) we consider only processes with the same final states (in source and detector) as in the SM

case. If additional processes are present, with different final states, the corresponding amplitudes have to be added incoherently to the rate [38].

We want to stress that our numerical results are not restricted only to the NSI resulting from the four-fermion operators discussed in Sec. III. The results apply to *all kinds of non-standard physics* in source, propagation and detection in a neutrino factory experiment, which can be parametrized as in Eqs. (26),(27),(32). In general the NSI parameter combinations involved in the quantum mechanical evolution of the neutrino system are model-dependent functions of the parameters appearing in the Lagrangian of a given theory, as discussed in Sec. II.

VI. THE OSCILLATION-NSI CONFUSION THEOREM

In this section we present analytical approximations for the transition rate and we show that within our simplified scenario NSI can lead to exactly the same signal at a neutrino factory as expected from genuine neutrino oscillations due to θ_{13}. Taking into account additional parameters like Δm_{sol}^2 or CP violating phases in the lepton mixing matrix or in NSI can only bring more serious complications for the determination of θ_{13} [14].

For the understanding of the physics relevant for the numerical results which we will present in the following sections it is useful to derive an analytic expression for the appearance rate Eq. (26). To this aim we assume a constant matter potential V and consider the terms containing the NSI parameters $\epsilon_{\alpha\beta}^P$ and s_{13} as a small perturbation of the Hamiltonian and calculate eigenvalues and eigenvectors of Eq. (32) up to first order in these small quantities. Then the appearance rate Eq. (26) is of second order in s_{13} and $\epsilon_{\alpha\beta}^X$ ($X = S, P, D$) and we make the interesting observation that only the three parameters $(s_{13}, \epsilon_{e\tau}^S, \epsilon_{e\tau}^P)$ appear.

This is a special feature of the $e \to \mu$ channel under the approximation (31) and can be understood from Fig. 1(a), where we show schematically the various contributions to this channel. The thick lines indicate the SM processes in source and detection and the dominating $\mu \leftrightarrow \tau$ oscillations due to atmospheric oscillation parameters. The thin lines show the leading contributions of small quantities, which involve only the parameters s_{13}, $\epsilon_{e\tau}^S$ and $\epsilon_{e\tau}^P$. With very thin lines we show some channels which involve more than one small quantity, and hence do not appear up to second order in the appearance rate: we consider only the detection of muons, therefore in leading order no effects of NSI in the detector show up because of Eq. (31). Similarly no FC effects in the $\tau \leftrightarrow \mu$ channel show up, since transitions from e to τ flavor already involve a small quantity, either s_{13} or $\epsilon_{e\tau}^{S,P}$. We also note that no NU coefficient $\epsilon_{\alpha\alpha}^X$ appears in leading order [34,35], explaining the lack of sensitivity of neutrino factory experiments to NU parameters [32].

Let us introduce the abbreviations

$$\epsilon_S \equiv \epsilon_{e\tau}^S, \quad \epsilon_P \equiv \epsilon_{e\tau}^P. \quad (34)$$

Then the expression for the appearance rate is a general quadratic form in the variables s_{13}, ϵ_S and ϵ_P:

---

[3]Note that in Ref. [35] much weaker sensitivities on FCI in the $e - \mu$ channel for the source at a neutrino factory are derived, of the order of 10^{-3}. A nonvanishing $\epsilon_{e\mu}^S$ would imply yet an additional source for the confusion of oscillations and NSI.
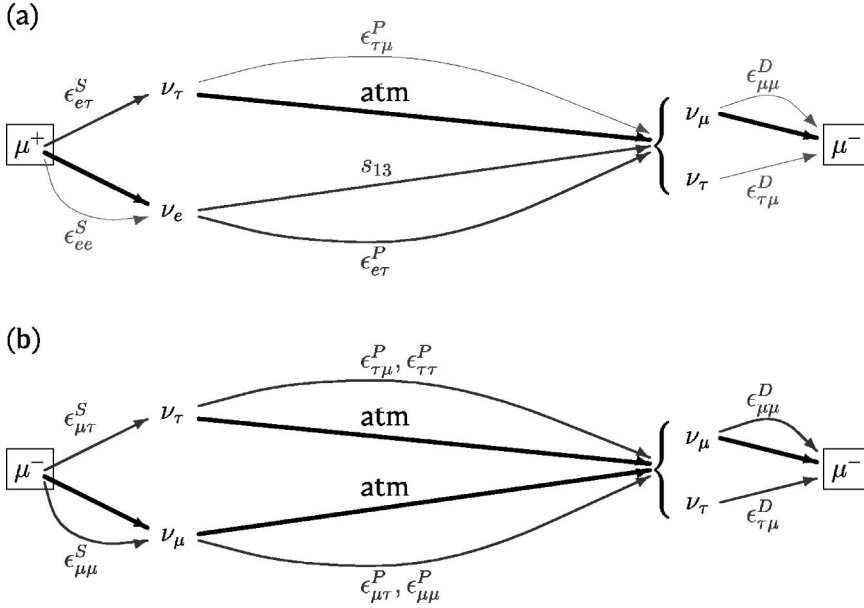
(a)

(b)

FIG. 1. NSI contributions to the (a) appearance and (b) disappearance channel in the approximation Eq. (31). The thick lines indicate the dominating processes, whereas the thin lines show the leading contributions of the small quantities s_{13} and $\epsilon_{\alpha\beta}^X$. The processes shown with very thin lines are double suppressed in small quantities.

$$\mathcal{R}_{e\mu} \approx A s_{13}^2 + B s_{13}\epsilon_P + C \epsilon_P^2 + D \epsilon_P\epsilon_S + E \epsilon_S^2 + F s_{13}\epsilon_S \qquad (35)$$

with the coefficients

$$A = 4 s_{23}^2 \left(\frac{\Delta}{\Delta - V}\right)^2 \sin^2 \frac{(\Delta - V)L}{2},$$

$$B = 4 s_{23}^2 c_{23}^2 r \frac{\Delta}{\Delta - V}$$
$$\times \left[\frac{\Delta + V}{\Delta - V}\sin^2 \frac{(\Delta - V)L}{2} + \sin^2 \frac{VL}{2} - \sin^2 \frac{\Delta L}{2}\right],$$

$$C = 4 s_{23}^2 c_{23}^2 r^2 \frac{\Delta}{\Delta - V}$$
$$\times \left[\frac{V}{\Delta - V}\sin^2 \frac{(\Delta - V)L}{2} + \sin^2 \frac{VL}{2} - \frac{V}{\Delta}\sin^2 \frac{\Delta L}{2}\right],$$

$$D = 4 s_{23}^2 c_{23}^2 r \frac{\Delta}{\Delta - V}$$
$$\times \left[\sin^2 \frac{(\Delta - V)L}{2} - \sin^2 \frac{VL}{2} - \left(1 - 2\frac{V}{\Delta}\right)\sin^2 \frac{\Delta L}{2}\right],$$

$$E = 4 s_{23}^2 c_{23}^2 \sin^2 \frac{\Delta L}{2},$$

$$F = 4 s_{23}^2 c_{23} \frac{\Delta}{\Delta - V}$$
$$\times \left[\sin^2 \frac{(\Delta - V)L}{2} - \sin^2 \frac{VL}{2} + \sin^2 \frac{\Delta L}{2}\right],$$

$$(36)$$

where L is the distance between neutrino source and detector. The appearance rate for anti-neutrinos $\mathcal{R}_{e\mu}^-$ is obtained by replacing $V \to -V$ in Eq. (36). These analytic expressions are in agreement with numerical calculations within a few % in the relevant parameter range. In general all coefficients $(A, \ldots, F)$ are of the same order of magnitude and depend on neutrino energy (via Δ), on the baseline and on the sign of V (neutrinos or anti-neutrinos) in a nontrivial way.

Performing a similar consideration for the μ disappearance channel one finds that the rate $\mathcal{R}_{\mu\mu}$, defined in a way similar to Eq. (26), contains terms of all powers of the small quantities. This is illustrated in Fig. 1(b). The zeroth order contribution corresponds to $\mu \leftrightarrow \tau$ oscillations with atmospheric neutrino oscillation parameters: in contrast to Fig. 1(a), in the case of Fig. 1(b) there is a channel involving only thick lines. However, we find that up to second order in small quantities only the parameters $(\epsilon_{\mu\tau}^S, \epsilon_{\mu\mu}^S, \epsilon_{\mu\tau}^P, \epsilon_{\mu\mu}^P, \epsilon_{\tau\tau}^P, \epsilon_{\tau\mu}^D, \epsilon_{\mu\mu}^D)$ appear. The important observation is that none of the three parameters $(s_{13}, \epsilon_{e\tau}^S, \epsilon_{e\tau}^P)$ relevant for the $e \to \mu$ channel appears. Therefore, no additional information on these parameters can be obtained by considering the disappearance channel. An analysis of this channel including all the parameters listed above goes beyond the scope of this paper and we will not consider it any further here.

Let us compare the transition rate for pure oscillations $(\epsilon_S = \epsilon_P = 0)$

$$\mathcal{R}_{e\mu}^{\text{osc}}(s_{13}) = A s_{13}^2 \qquad (37)$$

with the transition rate without oscillations $(s_{13} = 0)$ but nonzero NSI coefficients

$$\mathcal{R}_{e\mu}^{\text{NSI}}(\epsilon_S, \epsilon_P) = C \epsilon_P^2 + D \epsilon_P\epsilon_S + E \epsilon_S^2. \qquad (38)$$

With the expressions for A, C, D, E given in Eq. (36) it is easy to check that if the relation

$$\epsilon_S = r\epsilon_P \qquad (39)$$

holds, oscillations are indistinguishable from NSI. More precisely, we obtain

$$\mathcal{R}_{e\mu}^{\text{NSI}}(r\epsilon_P, \epsilon_P) = \mathcal{R}_{e\mu}^{\text{osc}}(s_{13}) \qquad (40)$$

with

$$s_{13}^2 = r^2 \epsilon_P^2 \frac{1 + \cos 2\theta_{23}}{2}. \tag{41}$$

This means that for each value of s_{13} there is a pair of NSI parameters (ϵ_S, ϵ_P) determined by Eqs. (39) and (41) which in our approximation leads to *exactly the same* signal as oscillations due to s_{13}. This includes both energy and baseline dependence, for both neutrinos and anti-neutrinos. We call this the "oscillation-NSI confusion theorem."

Of course, relation (39) represents a fine-tuning of the parameters ϵ_P and ϵ_S. However, as long as this relation cannot be excluded one has to consider this possibility. Moreover, in a realistic experiment with finite errors and statistical uncertainties there will be a *region* around the point in the (ϵ_S, ϵ_P) plane corresponding to Eqs. (39) and (41) in which oscillations cannot be distinguished from NSI.

VII. THE SIMULATION OF A NEUTRINO FACTORY EXPERIMENT

In our numerical calculations we assume a neutrino factory with an energy of 50 GeV for the stored muons and 2×10^{20} useful muon decays of each polarity per year for a period of 5 years. We consider a magnetized iron calorimeter with a mass of 40 kt. The neutrino detection threshold is set to 4 GeV, the energy resolution of the detector is approximated by a Gaussian resolution function with $\Delta E_\nu / E_\nu = 10\%$ and we use 20 bins in neutrino energy. We do not include any backgrounds, efficiencies and errors in the particle identification. The amplitude $\mathcal{A}_{\alpha\beta}^P$ describing the neutrino propagation is obtained by numerically solving the neutrino evolution equation with the Hamiltonian (32), using the average matter density along each baseline. In Ref. [58] it was shown that this is an excellent approximation as long as the baseline is shorter than approximately 10 000 km, i.e. as long as it does not cross the core. Then the transition rate Eq. (26) is folded with neutrino flux, cross section and energy resolution function to in order obtain the expected event rates in the detector. For further details see Refs. [14,59].

Our "observables" are the event rates for the appearance channel n_ν^i ($n_{\bar\nu}^i$) for neutrinos (anti-neutrinos) in each energy bin i. We fix the atmospheric oscillation parameters[4] at their best fit values given in [6,25] $\Delta m_{atm}^2 = 3 \times 10^{-3}$ eV^2 and $\sin^2 2\theta_{23} = 1$. Hence, at a given baseline, the event rates depend on the three parameters S_{13}, ϵ_S and ϵ_P, where we have introduced the abbreviation $S_{13} \equiv \sin^2 2\theta_{13}$.

In order to evaluate the impact of ϵ_S and ϵ_P on the capability of a neutrino factory to measure S_{13} we proceed as follows. To test a given point $(S_{13}^0, \epsilon_S^0, \epsilon_P^0)$ in the parameter space we calculate the event rates $(n_x^i)^0 \equiv n_x^i(S_{13}^0, \epsilon_S^0, \epsilon_P^0)$
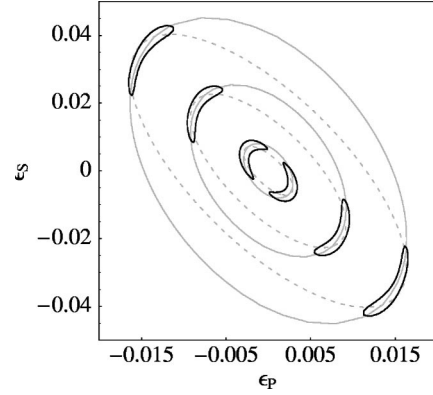

FIG. 2. Allowed regions at 90% C.L. (black solid lines) in the $S_{13} \equiv 0$ plane for three different starting values $S_{13}^0 = (3.2 \times 10^{-3}, 10^{-3}, 10^{-4})$ and $\epsilon_S^0 = \epsilon_P^0 = 0$ always. The baseline is 3 000 km. The gray lines indicate points with the same event rates as the starting point (gray solid for neutrinos, gray dashed for anti-neutrinos).

with $x = \nu, \bar\nu$ and construct a χ^2 appropriate for a Poisson distribution[5]:

$$\chi^2(S_{13}, \epsilon_S, \epsilon_P; S_{13}^0, \epsilon_S^0, \epsilon_P^0)$$

$$= 2 \sum_{x=\nu,\bar\nu} \sum_i \left[n_x^i(S_{13}, \epsilon_S, \epsilon_P) - (n_x^i)^0 \right.$$

$$\left. + (n_x^i)^0 \ln \frac{(n_x^i)^0}{n_x^i(S_{13}, \epsilon_S, \epsilon_P)} \right]. \tag{42}$$

Thus we obtain an allowed region in the three dimensional space $\mathcal{P}$ spanned by $(S_{13}, \epsilon_S, \epsilon_P)$ in the usual way. Note that the minimum of the χ^2 defined in Eq. (42) is zero and occurs at $(S_{13}, \epsilon_S, \epsilon_P) = (S_{13}^0, \epsilon_S^0, \epsilon_P^0)$. Therefore, the allowed region at the C.L. α is given by the set of all points in $\mathcal{P}$ which satisfy

$$\chi^2(S_{13}, \epsilon_S, \epsilon_P; S_{13}^0, \epsilon_S^0, \epsilon_P^0) \leq \Delta\chi_\alpha^2, \tag{43}$$

where $\Delta\chi_\alpha^2$ is determined by a χ^2 distribution with 3 degrees of freedom. For simplicity we consider only starting values with $\epsilon_S^0 = \epsilon_P^0 = 0$, i.e. pure oscillations.

VIII. SENSITIVITY LIMITS FOR $\sin^2 2\theta_{13}$

In Fig. 2 we show the allowed regions in the $S_{13} \equiv 0$ plane for a baseline of 3 000 km and three different starting values for S_{13}^0. In gray we show the lines with the same total event rates (solid for neutrinos, dashed for anti-neutrinos) as in the starting point. The general shape of these lines can immediately be understood from Eq. (35). The small regions delimited by the dark solid lines arise from a global fit procedure including also the information on the spectra with the ex-

---

[4]They will be determined at the neutrino factory with high accuracy from the disappearance channel.

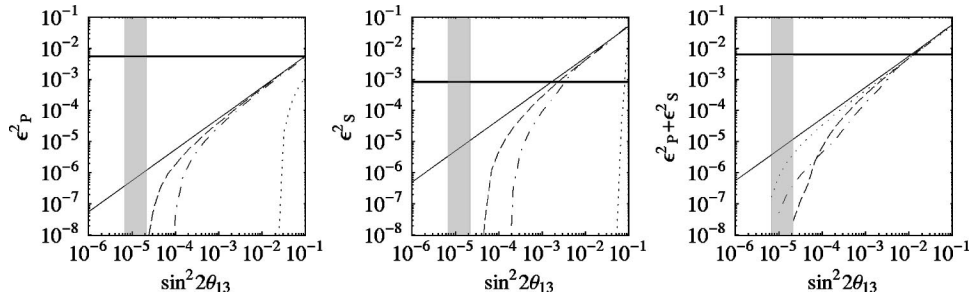[5]We are dealing with a counting experiment with eventually very low counts.

FIG. 3. Sensitivity limits at 90% C.L. on $\sin^2 2\theta_{13}$ attainable if a bound on ϵ_P^2 (left panel), ϵ_S^2 (middle panel) or $\epsilon_P^2 + \epsilon_S^2$ (right panel) is given. The dotted line is for a baseline of 700 km, the dash-dotted line for 3000 km and the dashed line for 7000 km. The horizontal black line illustrates the order of magnitude of current limits on the NSI parameter in order to "guide the eye." The vertical gray band shows the range of possible sensitivities without NSI [14]. The diagonal solid line is the theoretical bound derived from our confusion theorem.

pected energy resolution as described above. One notices that these confidence regions follow closely the intersection of the lines of constant rates for neutrinos and anti-neutrinos. This means that most information is obtained from simultaneously taking into account neutrino and anti-neutrino rates [33]. This follows from the fact that the allowed regions extend as long as the lines of constant neutrino and anti-neutrino rate are close to each other, i.e. *both* rates are similar to the ones in the test point. We conclude that it is important to run the neutrino factory in both polarities. On the other hand we learn that most of the information is contained in the total rates; the spectral information is not very important: our results are rather insensitive to variations of the number of energy bins and of the energy resolution assumed.

Solutions in the $S_{13} \equiv 0$ plane of the type as shown in Fig. 2 *always* exist, irrespective of the starting value S_{13}^0. This is a consequence of the confusion theorem we have presented in Sec. VI. However, the magnitude of the required NSI parameters ϵ_S and ϵ_P strongly depends on the size of S_{13}^0 as can be seen from Eq. (41) or Fig. 2. Thus, *it is only possible to derive a limit on S_{13} if there is a limit on ϵ_S and/or ϵ_P*; a neutrino factory can only test a certain value of S_{13} if the values of ϵ_S and/or ϵ_P, which lead to the same signal, are ruled out by some other measurement. In Fig. 3 we show the attainable sensitivity limit on S_{13} as a function of different limits on the NSI parameters (the present estimated NSI limits are indicated by the solid horizontal lines). We define this sensitivity on S_{13} in the following way. For a dense grid of starting values S_{13}^0 in the range $10^{-6} - 10^{-1}$ we calculate the 90% C.L. allowed region in the $S_{13} \equiv 0$ plane as shown in Fig. 2. For each value of S_{13}^0 we show the minimum value of ϵ_P^2 (left panel), ϵ_S^2 (middle panel) or $\epsilon_P^2 + \epsilon_S^2$ (right panel) inside this allowed region. The neutrino factory is sensitive to this value of S_{13} only if there is a bound on this NSI parameter (combination of parameters), which is smaller than this minimum value.

Any experiment (e.g. like a near detector at a neutrino factory) trying to measure ϵ_S and ϵ_P will only restrict a certain combination of the NSI parameters in the source and the detector used in this particular experiment [see Eq. (33)]. In general it will be very difficult to translate such a result into a bound on ϵ_S, and even more difficult on ϵ_P, in a model-independent way. It is however to be expected that the constrained combination depends on the square of the NSI

parameters since the transition rate $\mathcal{R} \propto \epsilon^2$. Therefore we show the results for the three simple functions ϵ_S^2, ϵ_P^2 and $\epsilon_S^2 + \epsilon_P^2$ as mentioned above. The left hand panel of Fig. 3 shows the sensitivity limit if there is a bound on ϵ_P^2 and all values of ϵ_S are allowed. It seems very difficult to obtain such a bound in a model-independent way, because it is not possible to probe directly the NSI parameters relevant in neutrino propagation. As recently stressed in Ref. [56] in general it is not possible to use bounds on similar processes involving charged leptons. Moreover, many different processes may contribute to ϵ_P [see Eq. (29)]. In the middle panel we show the sensitivity limits for a bound on ϵ_S^2 and all values allowed for ϵ_P, which is probably the most realistic case because it should be possible to constrain ϵ_S with a near detector setup. In the right hand panel we display the optimal situation, if a bound on the combination $\epsilon_S^2 + \epsilon_P^2$ is available.

The diagonal solid line in Fig. 3 shows the theoretical bound implied by the oscillation–NSI confusion theorem Eqs. (39) and (41). This bound corresponds to the best possible situation, which can be achieved only for large values of S_{13} due to large event numbers. For smaller values of S_{13} the realistic bound gets worse because of statistical limitations due to small event numbers. The numerical differences between the three plots in Fig. 3 is due to the different symmetries of the used function of ϵ_S and ϵ_P with respect to the symmetry of the allowed regions in the $S_{13} \equiv 0$ plane. For small values of $\epsilon_S^2 + \epsilon_P^2$ (right panel) the bounds converge to the sensitivity limits obtained without taking into account NSI [14]. The range of these limits for the three different baselines is shown as the gray vertical band.

We can understand the behavior of the sensitivity limits in Fig. 3 by considering the allowed regions in the $S_{13} \equiv 0$ plane for different baselines, as shown in Fig. 4. For small baselines the allowed region is roughly a circle. Therefore a bound on an individual ϵ_P or ϵ_S is useless for a sensitive determination of S_{13} (see left and middle panel of Fig. 3). We conclude that if only a baseline of 700 km is available it is mandatory to establish solid bounds on *both* NSI parameters. However, a bound on $\epsilon_P^2 + \epsilon_S^2$ is most suitable for small baselines and in this case $L = 700$ km can do even better than longer baselines (right panel of Fig. 3). For longer baselines the allowed regions in the $S_{13} \equiv 0$ plane become smaller (see
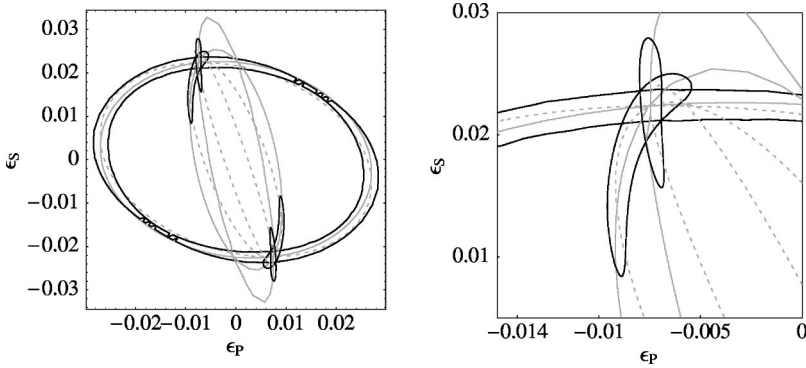
FIG. 4. Allowed regions at 90% C.L. (black solid lines) in the $S_{13} \equiv 0$ plane for three different baselines ($L = 1000$ km, 3000 km, 5000 km) and $S_{13}^0 = 10^{-3}$, $\epsilon_S^0 = \epsilon_P^0 = 0$. The gray lines indicate points with the same event rates as the starting point (gray solid for neutrinos, gray dashed for anti-neutrinos). The right-hand panel is a blow up of the left-hand panel.

Fig. 4) and hence, also a bound on an individual NSI parameter is useful.

With the solid horizontal lines in Fig. 3 we illustrate the order of magnitude of current bounds on NSI parameters. For ϵ_P we show the bound given in Eq. (24), while for the ϵ_S case we use the bound given in Eq. (23). It is clearly visible that using even these rather optimistic bounds on the relevant NSI parameters the sensitivity of a neutrino factory is at its best $S_{13} \sim 10^{-3}$—compared to $S_{13} \sim 10^{-5}$—in the absence of any NSI. The sensitivity is deteriorated by two orders of magnitude for all baselines. Let us stress again that we are *not* using the bounds from Eqs. (24) and (23) in our analysis because they are derived under some model-dependent assumptions from non-neutrino processes. The horizontal lines in Fig. 3 should merely "guide the eye" in reading the plots, they simply give a rough idea of the order of magnitude of existing bounds.

The geometry of the currently discussed muon storage rings offers the striking possibility to illuminate two detectors at different baselines with neutrinos from one neutrino factory. With this in mind, let us investigate to which extent the sensitivities for S_{13} can be improved by combining the information of two baselines. From Fig. 4 we find that although the shape of the allowed regions in the $S_{13} \equiv 0$ plane is very different for different baselines, they all have a common intersection. Moreover, considering the lines in the $S_{13} \equiv 0$ plane which have the same event rates as the starting value S_{13}^0 (shown as gray solid lines for neutrinos and gray dashed lines for anti-neutrinos) we observe that all iso-rate lines meet in a single point. This is again due to our

oscillation–NSI confusion theorem: Eqs. (39) and (41) do not depend on the baseline. Thus even the combination of baselines cannot lift this degeneracy.

In Fig. 5 we show sensitivity limits for S_{13} obtained as before, but now we use the sum of the χ^2-functions Eq. (42) for two different baselines. In comparison with Fig. 3 we observe that the theoretical bound can now be achieved somewhat easier. However, in contrast to the case considered in our previous work [33], where only NSI with the earth matter are taken into account, in our present more realistic situation including also effects in the neutrino source even a combination of baselines does not resolve the confusion problem. With the current bounds on the relevant NSI parameters the sensitivity is $S_{13} \gtrsim 10^{-3}$, which coincides with the sensitivity obtained at a single baseline. Again this sensitivity is two orders of magnitude worse than without NSI.

IX. CONCLUSIONS

In this paper we have considered the impact of nonstandard neutrino interactions on the determination of neutrino mixing parameters at a neutrino factory. In particular we have focused on the so-called "golden channels" for the measurement of θ_{13}, namely the $\overset{(-)}{\nu}_e \rightarrow \overset{(-)}{\nu}_\mu$ channels. We have extended our previous work [33] by taking into account both the effects of neutrino oscillations as well as the effect of NSI at the neutrino source, propagation and detection [38]. Within a very good approximation we have explicitly demonstrated how a certain combination of FC interactions in source and propagation can produce exactly the same sig-
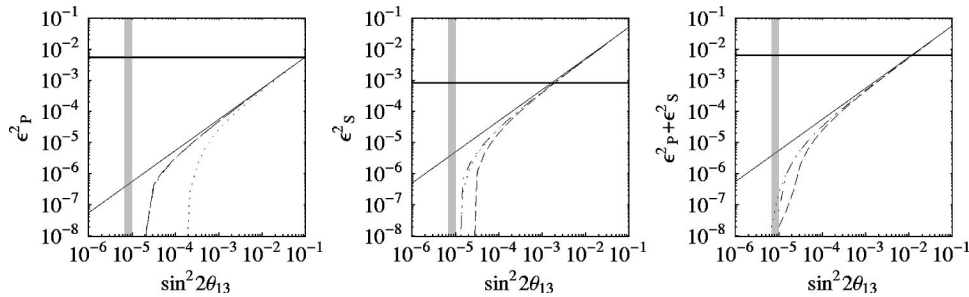

FIG. 5. Sensitivity limits at 90% C.L. on $\sin^2 2\theta_{13}$ attainable if a bound on ϵ_P^2 (left panel), ϵ_S^2 (middle panel) or $\epsilon_P^2 + \epsilon_S^2$ (right panel) is given. The dotted line is for the baseline combination 700 km and 3000 km, the dash-dotted line for 700 km and 7000 km and the dashed line for 3000 km and 7000 km. The horizontal black line illustrates the order of magnitude of existing limits on the NSI parameter. The vertical gray band shows the range of possible sensitivities without NSI [14]. The diagonal solid line is the theoretical bound derived from the confusion theorem.

nal as would be expected from oscillations arising due to θ_{13}. This implies that information about θ_{13} can only be obtained if bounds on NSI parameters are available and that all one can achieve at a neutrino factory is a *correlated oscillation-NSI study*. In view of the current estimates of the bounds on FC interactions, this leads to a drastic loss in sensitivity in θ_{13}, at least two orders of magnitude.

In order to improve the situation it is mandatory to obtain better bounds on ϵ_S and ϵ_P at the $\epsilon \simeq 10^{-4} - 10^{-3}$ level, which is several orders of magnitude more stringent than current limits. This unexpected complication should be taken into account in the design of a neutrino factory. On the other hand, a neutrino factory may also offer the possibility to obtain these very stringent limits on the NSI parameters. Us-

ing a small near detector ($L \approx 100$ m) with very good particle identification for taus it would be possible to restrict the $\mathcal{R}_{e\tau}$ down to $10^{-8} - 10^{-6}$. Since $\mathcal{R}_{e\tau} \propto \epsilon^2$ this translates into a bound for $\epsilon \simeq 10^{-4} - 10^{-3}$ [57]. Thus the near site physics program of a neutrino factory is a necessary and very important part of the long baseline program.

[1] B. T. Cleveland *et al.*, Astrophys. J. **496**, 505 (1998); Kamiokande Collaboration, K.S. Hirata *et al.*, Phys. Rev. Lett. **77**, 1683 (1996); GALLEX Collaboration, W. Hampel *et al.*, Phys. Lett. B **447**, 127 (1999); SAGE Collaboration, D.N. Abdurashitov *et al.*, Phys. Rev. Lett. **83**, 4686 (1999); Super-Kamiokande Collaboration, Y. Fukuda *et al.*, *ibid.* **81**, 1158 (1998); SNO Collaboration, Q.R. Ahmad, *et al.*, *ibid.* **87**, 071301 (2001).

[2] Super-Kamiokande Collaboration, Y. Fukuda *et al.*, Phys. Rev. Lett. **81**, 1562 (1998); Kamiokande Collaboration, Y. Fukuda *et al.*, Phys. Lett. B **335**, 237 (1994); IMB Collaboration, R. Becker-Szendy *et al.*, Nucl. Phys. B (Proc. Suppl.) **38**, 331 (1995); Soudan Collaboration, W.W.M. Allison *et al.*, Phys. Lett. B **449**, 137 (1999); MACRO Collaboration, M. Ambrosio *et al.*, *ibid.* **434**, 451 (1998).

[3] LSND Collaboration, C. Athanassopoulos *et al.*, Phys. Rev. Lett. **77**, 3082 (1996); **81**, 1774 (1998); LSND Collaboration, A. Aguilar *et al.*, Phys. Rev. D **64**, 112007 (2001).

[4] J. T. Peltoniemi, D. Tommasini, and J.W. Valle, Phys. Lett. B **298**, 383 (1993); D.O. Caldwell and R.N. Mohapatra, Phys. Rev. D **48**, 3259 (1993); J.T. Peltoniemi and J.W. Valle, Nucl. Phys. **B406**, 409 (1993).

[5] M. Maltoni, T. Schwetz, and J.W. Valle, Phys. Rev. D **65**, 093004 (2002).

[6] M.C. Gonzalez-Garcia, M. Maltoni, C. Peña-Garay, and J.W.F. Valle, Phys. Rev. D **63**, 033005 (2001).

[7] J. Schechter and J.W. Valle, Phys. Rev. D **22**, 2227 (1980).

[8] J. Schechter and J.W. Valle, Phys. Rev. D **23**, 1666 (1981).

[9] M.C. Gonzalez-Garcia, P.C. de Holanda, C. Pena-Garay, and J.W. Valle, Nucl. Phys. **B573**, 3 (2000).

[10] J.N. Bahcall, *et al.*, J. High Energy Phys. **08**, 014 (2001); G.L. Fogli *et al.*, Phys. Rev. D **64**, 093007 (2001); P.I. Krastev and A.Yu. Smirnov, *ibid.* **65**, 073022 (2002); P. Creminelli, G. Signorelli, and A. Strumia, J. High Energy Phys. **05**, 052 (2001); A. Bandyopadhyay *et al.*, Phys. Lett. B **519**, 83 (2001).

[11] KamLAND web page: http://www.awa.tohoku.ac.jp/html/KamLAND/index.html

[12] CHOOZ Collaboration, M. Apollonio *et al.*, Phys. Lett. B **466**, 415 (1999); Palo Verde Collaboration, F. Boehm *et al.*, Phys. Rev. D **64**, 112001 (2001).

[13] C. Quigg, Nucl. Instrum. Methods Phys. Res. A **451**, 1 (2000); C. Albright *et al.*, hep-ex/0008064; B. Autin *et al.*, CERN-SPSC-98-30; S. Geer, Phys. Rev. D **57**, 6989 (1998); **59**, 039903(E) (1998).

[14] M. Freund, P. Huber, and M. Lindner, Nucl. Phys. **B615**, 331 (2001); A. Cervera *et al.*, *ibid.* **B579**, 17 (2000); **B593**, 731(E) (2000).

[15] G.G. Ross and J.W.F. Valle, Phys. Lett. **151B**, 375 (1985); J.R. Ellis *et al.*, *ibid.* **150B**, 142 (1985); A. Masiero and J.W. Valle, Phys. Lett. B **251**, 273 (1990).

[16] L.J. Hall and M. Suzuki, Nucl. Phys. **B231**, 419 (1984); M.A. Diaz, J.C. Romao, and J.W.F. Valle, *ibid.* **B524**, 23 (1998); R. Hempfling, *ibid.* **B478**, 3 (1996).

[17] R.N. Mohapatra and J.W. Valle, Phys. Rev. D **34**, 1642 (1986).

[18] L.J. Hall, V.A. Kostelecky, and S. Raby, Nucl. Phys. **B267**, 415 (1986).

[19] L. Wolfenstein, Phys. Rev. D **17**, 2369 (1978); S.P. Mikheev and A.Yu. Smirnov, Sov. J. Nucl. Phys. **42**, 913 (1985).

[20] J.W.F. Valle, Phys. Lett. B **199**, 432 (1987).

[21] M. Guzzo, A. Masiero, and S. Petcov, Phys. Lett. B **260**, 154 (1991); E. Roulet, Phys. Rev. D **44**, 935 (1991); V. Barger, R.J.N. Phillips, and K. Whisnant, *ibid.* **44**, 1629 (1991); S. Bergmann, Nucl. Phys. **B515**, 363 (1998); E. Ma and P. Roy, Phys. Rev. Lett. **80**, 4637 (1998).

[22] S. Bergmann, M.M. Guzzo, P.C. de Holanda, P.I. Krastev, and H. Nunokawa, Phys. Rev. D **62**, 073001 (2000).

[23] M. Guzzo, P.C. de Holanda, M. Maltoni, H. Nunokawa, M.A. Tortola, and J.W.F. Valle, Nucl. Phys. **B629**, 479 (2002).

[24] M.C. Gonzalez-Garcia *et al.*, Phys. Rev. Lett. **82**, 3202 (1999); N. Fornengo, M.C. Gonzalez-Garcia, and J.W.F. Valle, J. High Energy Phys. **07**, 006 (2000); P. Lipari and M. Lusignoli, Phys. Rev. D **60**, 013003 (1999); G.L. Fogli, E. Lisi, A. Marrone, and G. Scioscia, Phys. Rev. D **60**, 053006 (1999).

[25] N. Fornengo, M. Maltoni, R. Tomas, and J.W.F. Valle, Phys. Rev. D **65**, 013010 (2002).

[26] S. Bergmann, Y. Grossman, and D.M. Pierce, Phys. Rev. D **61**, 053005 (2000).

[27] H. Nunokawa, Y.Z. Qian, A. Rossi, and J.W.F. Valle, Phys. Rev. D **54**, 4356 (1996); D. Grasso, H. Nunokawa, and J.W.F. Valle, Phys. Rev. Lett. **81**, 2412 (1998).

[28] H. Nunokawa, A. Rossi, and J.W.F. Valle, Nucl. Phys. **B482**, 481 (1996).

[29] S. Bergmann and Y. Grossman, Phys. Rev. D **59**, 093005 (1999).

[30] S. Bergmann, H.V. Klapdor-Kleingrothaus, and H. Pas, Phys. Rev. D **62**, 113002 (2000).

[31] Z. Berezhiani, R.S. Raghavan, and A. Rossi, hep-ph/0111138.

[32] P. Huber and J.W.F. Valle, Phys. Lett. B **523**, 151 (2001).

[33] P. Huber, T. Schwetz, and J.W. Valle, Phys. Rev. Lett. **88**, 101804 (2002).

[34] A.M. Gago, M.M. Guzzo, H. Nunokawa, W.J. Teves, and R. Zukanovich Funchal, Phys. Rev. D **64**, 073003 (2001).

[35] M.C. Gonzalez-Garcia, Y. Grossman, A. Gusso, and Y. Nir, Phys. Rev. D **64**, 096006 (2001).

[36] A. Datta, R. Gandhi, B. Mukhopadhyaya, and P. Mehta, Phys. Rev. D **64**, 015011 (2001).

[37] L.M. Johnson and D.W. McKay, Phys. Rev. D **61**, 113007 (2000).

[38] T. Ota, J. Sato, and N. Yamashita, Phys. Rev. D **65**, 093015 (2002).

[39] A. Bueno, M. Campanelli, M. Laveder, J. Rico, and A. Rubbia, J. High Energy Phys. **06**, 032 (2001).

[40] Y. Itow *et al.*, hep-ex/0106019; VLBL Study Group H2B-4 Collaboration, Y.F. Wang *et al.*, Phys. Rev. D **65**, 073021 (2002); V. Barger, D. Marfatia, and K. Whisnant, *ibid.* **65**, 073023 (2002); V.D. Barger *et al.*, *ibid.* **65**, 053016 (2002); H. Minakata and H. Nunokawa, J. High Energy Phys. **10**, 001 (2001).

[41] M. Gell-Mann, P. Ramond, and R. Slansky, in *Supergravity*, edited by P. van Niewenhuizen and D. Freedman (North-Holland, Amsterdam, 1979); T. Yanagida, in *KEK Lectures*, edited by O. Sawada and A. Sugamoto (KEK, Tsukuba, 1979); R.N. Mohapatra and G. Senjanovic, Phys. Rev. Lett. **44**, 912 (1980).

[42] M.C. Gonzalez-Garcia and J.W.F. Valle, Phys. Lett. B **216**, 360 (1989).

[43] J. Bernabeu, A. Santamaria, J. Vidal, A. Mendez, and J.W.F. Valle, Phys. Lett. B **187**, 303 (1987).

[44] M.C. Gonzalez-Garcia, A. Santamaria, and J.W.F. Valle, Nucl. Phys. **B342**, 108 (1990); M. Dittmar, A. Santamaria, M.C. Gonzalez-Garcia, and J.W.F. Valle, *ibid.* **B332**, 1 (1990).

[45] N. Rius and J.W.F. Valle, Phys. Lett. B **246**, 249 (1990).

[46] J.W.F. Valle, Prog. Part. Nucl. Phys. **26**, 91 (1991).

[47] M.C. Gonzalez-Garcia and J.W.F. Valle, Mod. Phys. Lett. A **7**, 477 (1992); A. Ilakovac, Phys. Rev. D **62**, 036010 (2000).

[48] M. Hirsch *et al.*, Phys. Rev. D **62**, 113008 (2000); **61**, 071703 (2000).

[49] M. Fukugita and T. Yanagida, Phys. Lett. B **206**, 93 (1988).

[50] R. Barbieri, L. Hall, and A. Strumia, Nucl. Phys. **B445**, 219 (1995).

[51] Particle Data Group, D.E. Groom *et al.*, Eur. Phys. J. C **15**, 1 (2000).

[52] P. Langacker and D. London, Phys. Rev. D **39**, 266 (1989).

[53] Y. Grossman, Phys. Lett. B **359**, 141 (1995).

[54] S.N. Gninenko, M.M. Kirsanov, N.V. Krasnikov, and V.A. Matveev, hep-ph/0106302.

[55] CHORUS Collaboration, E. Eskut *et al.*, Phys. Lett. B **497**, 8 (2001).

[56] Z. Berezhiani and A. Rossi, hep-ph/0111137.

[57] M.L. Mangano *et al.*, hep-ph/0105155.

[58] M. Freund and T. Ohlsson, Mod. Phys. Lett. A **15**, 867 (2000).

[59] M. Freund, P. Huber, and M. Lindner, Nucl. Phys. **B585**, 105 (2000).